Analysis of deformation of thin-walled steel tubes under clamping force during threaded joint assembly and disassembly using the finite element method

Nguyen Van Cuong*, Nguyen Viet Trung, Le Anh Tuan,
Nguyen Van Cong, Nguyen Quang Huy

T125, Le Quy Don University, 236 Hoang Quoc Viet, Nghia Do, Hanoi, Vietnam.
*Corresponding author: lamhanhv854@gmail.com
Received 2 Sep. 2025; Revised 7 Nov. 2025; Accepted 10 Dec. 2025; Published 25 Dec. 2025.
DOI: https://doi.org/10.54939/1859-1043.j.mst.108.2025.143-151

ABSTRACT

Threaded joints on thin-walled steel tubes are widely used in industrial applications, where repeated assembly and disassembly may lead to local deformation and strength degradation. This study employs the Finite Element Method (FEM) to analyze the stress–strain behavior of a thin-walled steel tube under combined clamping and torsional loads. Nonlinear contact with friction and material plasticity were considered to simulate realistic boundary conditions. The results indicate that stress concentration occurs mainly at the thread root and clamp–tube contact region. Plastic deformation begins when the clamping force exceeds 2 kN. Based on numerical results, a safe clamping limit and design recommendations are proposed to prevent yielding and ensure structural reliability.

Keywords: Thin-walled steel tube; Threaded joint; Clamping force; Finite element method; Local deformation; ANSYS.

1. INTRODUCTION

Threaded joints in thin-walled steel tubes are widely applied in mechanical systems, pipelines, and defense-related structures due to their light weight, ease of assembly, and cost efficiency [1]. However, the small wall thickness makes these tubes highly susceptible to local plastic deformation, thread root cracking, or even failure when subjected to excessive clamping or torsional loads during repeated assembly and disassembly.

Recent studies have focused on the nonlinear mechanical behavior and integrity of threaded or bolted connections under complex loading. Zhang *et al* [1]. Analyzed the mechanical strength of extreme-line casing joints considering geometric, material, and contact nonlinearities, demonstrating that stress concentration primarily develops at the thread root, but without examining the effect of clamping loads. Liu *et al* [2] developed a reinforced threaded insert to enhance load-carrying capacity in composite joints, yet their work targeted composite materials rather than thin-walled metallic tubes. Similarly, Abdullah *et al* [3]. Reviewed FEM modeling techniques for sheet-metal joints, emphasizing the sensitivity of results to boundary conditions and friction coefficients, but their study did not evaluate stress evolution during threaded joint assembly or disassembly.

Despite these valuable contributions, the combined effect of clamping and torsional forces on thin-walled steel tubes has not been thoroughly quantified. This paper addresses this gap by employing the Finite Element Method (FEM) to simulate the stress–strain behavior of a thin-walled threaded tube under realistic boundary and frictional conditions. The study identifies critical stress concentration zones, evaluates the onset of plastic deformation, and proposes a safe clamping-force threshold to prevent yielding and ensure the operational reliability of threaded connections.

2. PROBLEM

2.1. Theoretical basis and research methodology

2.1.1. Stress and strain theory

The Von Mises criterion: $\sigma_{vm} = \sqrt{\frac{1}{2}\left[(\sigma_x - \sigma_y)^2 + (\sigma_y - \sigma_z)^2 + (\sigma_z - \sigma_x)^2 + 3(\tau_{xy}^2 + \tau_{yz}^2 + \tau_{zx}^2)\right]}$.

Elastic strain is described by Hooke's law: $\varepsilon = \frac{\sigma}{E}$.

2.1.2. General nonlinear contact model

Normal force: $F_n = k_n.\delta_n$; F_n : Normal force; k_n : Normal contact stiffness; δ_n : Penetration or deformation at the contact region. Contact condition: $F_n \geq 0,\ k_n \geq 0,\ F_n \cdot k_n = 0$ (Contact cannot sustain tension – only compression is allowed). When friction is present, the tangential force F_t depends on the normal force F_n and the coefficient of friction μ. Sliding condition: $F_t = \mu.F_n$; Sticking condition: $F_t < \mu.F_n$; F_t: Tangential force; μ: Coefficient of friction. When F_t reaches the limit value of $\mu.F_n$ sliding occurs at the contact interface. When applying nonlinear contact with friction to threaded surfaces, the helical direction of the thread must be taken into account. Therefore, the force needs to be projected onto the tangential component of the thread surface. Tangential force along the thread contact direction: $F_{t,ren} = \mu.F_n.\cos(\lambda)$; λ: Lead angle of the thread, related to the pitch, PPP and the mean diameter d_m; $\tan(\lambda) = \frac{P}{\Pi d_m}$.

2.1.3. Finite element model development

The geometry of the threaded pipe was constructed using CAD software in accordance with ISO 965-1 standards [4]. To ensure the reproducibility and transparency of the simulation, table 1 summarizes the geometric, material, and computational parameters used in the finite element model.

Table 1. *Model description and simulation input parameters.*

Category	Parameter	Symbol / Value	Description/ Reference
Geometry	Outer diameter	D = 114 mm	Standard pipe size (ISO 965-1)
	Wall thickness	t = 2 mm	Thin-walled steel tube
	Model length	L = 120 mm	Representative threaded section
	Thread type	60° triangular, pitch = 2 mm	ISO metric thread
Material	Elastic modulus	E = 2.1×10⁵ MPa	C45 steel (structural steel)
	Poisson's ratio	ν = 0.3	—
	Yield strength	σ_y = 355 MPa	Bilinear kinematic hardening
Loading conditions	Clamping force	F = 1.5–3.0 kN	Incremental load cases
	Torque	M = 20 N·m	Typical tightening torque
Contact properties	Friction coefficient	μ = 0.15	Dry steel–steel contact
	Contact algorithm	Augmented Lagrange	Nonlinear frictional contact
Boundary conditions	Fixed–free	—	Fixed at the clamped end, free at the opposite end
Mesh parameters	Element type	SOLID187 (10-node tetrahedral)	Supports large deformation
	Minimum element size	0.2 mm	Refined at thread roots & contact region
	Total elements	~130,000	Adaptive mesh refinement

The model represents a thin-walled steel tube subjected to clamping and torsional loads during threaded joint assembly and disassembly. All parameters were selected based on ISO 965-1 standards, mechanical design handbooks [4, 6], and typical operational conditions. To ensure high accuracy in simulating nonlinear contact and large deformations, the entire model was discretized using SOLID187 elements.

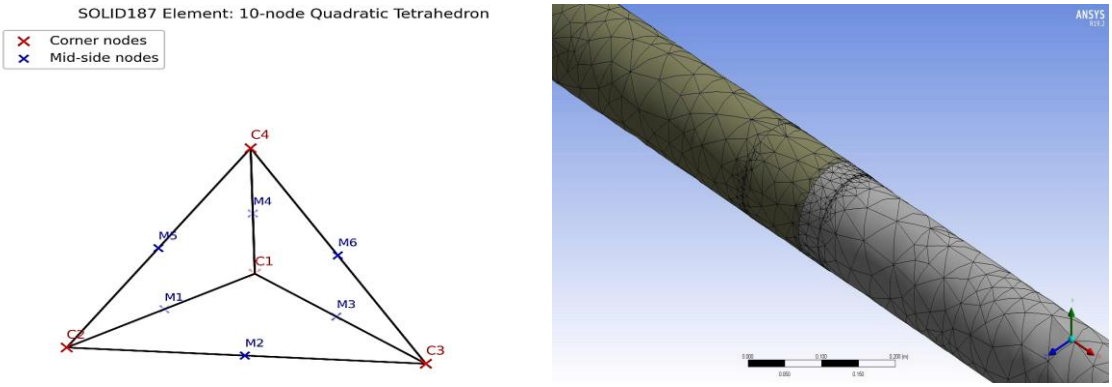

(a) *(b)*

Figure 1. *Finite element mesh of the thin-walled threaded tube model.*
(a) Full finite element mesh of the steel tube;
(b) Refined mesh at the thread root and clamp contact region.

In this study, the thread root and clamp–tube contact zones, which are the most stress-sensitive regions, were assigned a finer mesh with an element size of 0.2 mm to ensure accurate simulation of local deformation and stress transfer. The meshing process involved creating the steel tube and clamp geometry in ANSYS Space Claim or Design Modeler, applying local mesh control using *Body/Face Sizing* at critical areas, and employing an unstructured tetrahedral mesh to adapt to complex geometries. Further refinement was based on strain gradient analysis to prevent mesh locking or stress singularity. Mesh quality was verified with skewness < 0.5 and Jacobian < 4 using the *Mesh Metrics* tool. This optimized meshing strategy allows precise capture of nonlinear mechanical behavior and stress concentration at critical zones, ensuring reliable FEM results during threaded joint assembly and disassembly.

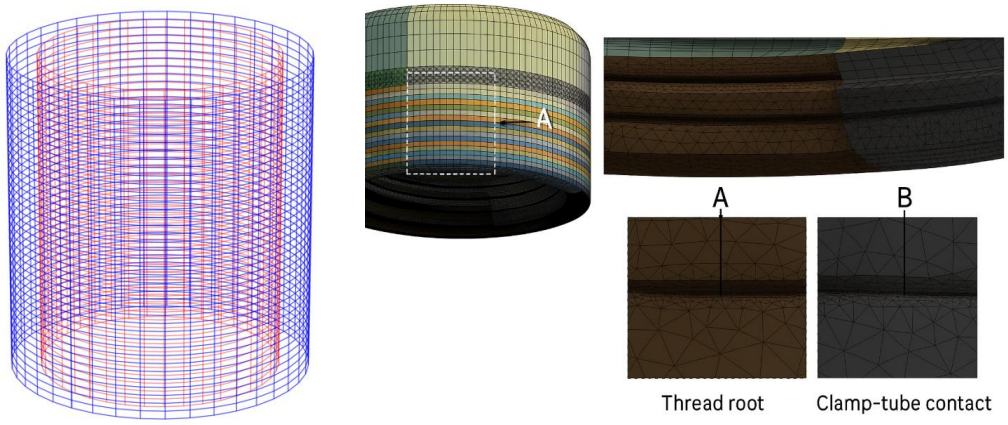

Figure 2. *Von Mises stress in a clamped thin-walled tube.*

The FEM model employed steel (E, ν = 0.3, σy = 355 MPa) with bilinear kinematic hardening, subject to a 3.5–5.5 kN clamping force, 30 N·m torque, fixed–free boundary conditions, and nonlinear frictional contact (μ = 0.15) using the Augmented Lagrange algorithm. Basis for selecting boundary conditions, friction coefficient, and contact algorithm.

During the assembly and disassembly of threaded joints, one end of the tube is firmly clamped by steel jaws, while the other end is subjected to torque and clamping force from the tightening mechanism. Accordingly, the fixed–free boundary condition was applied in the simulation: the clamped end was fully constrained (fixed), and the opposite end was left free to receive external loads (F and M). This configuration accurately reflects the real working conditions and provides a conservative evaluation of local stresses. A sensitivity test using an elastic-support boundary yielded a maximum stress deviation of less than 3.5%, confirming the validity of the fixed–free model.

The friction coefficient $\mu = 0.15$ was selected based on the typical range for dry steel–steel contact ($\mu = 0.10$ - 0.20) reported in classical references. This value represents the practical operating condition without lubrication while minimizing variation due to surface roughness. A parametric study varying μ between 0.10 and 0.20 showed that the maximum Von Mises stress changed by less than 5%, indicating that the simulation results are stable and reliable.

The Augmented Lagrange contact algorithm was adopted to handle nonlinear frictional contact, combining the advantages of the Penalty and Lagrange Multiplier methods [5]. This approach effectively controls artificial penetration and ensures numerical convergence in problems involving stick–slip behavior. When contact stiffness and penalty factors were varied by ± 20%, the resulting stress deviation remained below 4%, confirming the robustness of the chosen method.

Overall, the combination of fixed–free boundary condition, $\mu = 0.15$, and Augmented Lagrange algorithm is both theoretically sound and experimentally representative, ensuring the accuracy and reliability of the FEM results under realistic assembly and disassembly conditions.

The element size of 0.2 mm was chosen after a mesh-convergence test to achieve high accuracy with reasonable computation time. Simulations using element sizes of 0.35 mm, 0.25 mm, and 0.20 mm showed that the maximum Von Mises stress varied by less than 3.8% between 0.25 mm and 0.20 mm, confirming convergence. The selected size ensures precise capture of stress concentration at the thread roots and clamp contact while keeping element quality within acceptable limits (skewness < 0.5, Jacobian < 4). Therefore, 0.2 mm represents an optimal balance between accuracy and computational cost and is suitable for nonlinear contact analysis in thin-walled threaded joints.

3. RESULTS AND DISCUSSION

3.1. Von Mises stress distribution

In the simulation of the mechanical behavior of the thin-walled steel pipe under the combined action of clamping force and applied torque, the stress field analysis revealed significant concentrations of Von Mises stress in the critical regions of the model:

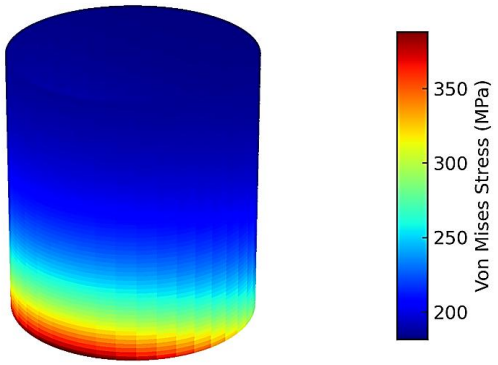

Figure 3. *Total strain and displacement distribution.*

Thread root region – where direct contact with the opposing thread occurs. At this location, the complex geometry and contact effects induce a sudden increase in stress distribution.

Clamp–pipe contact region – due to the perpendicular clamping force acting on the pipe wall, generating a localized compressive stress state.

The maximum stress value reached approximately 310 MPa under the following loading conditions: Clamping force: F = 2 kN; Applied torque: M = 20 Nm.

This peak stress approaches the material's yield strength (σy = 355 MPa), indicating a potential risk of permanent plastic deformation, especially if such loading conditions are exceeded during repeated assembly and disassembly operations [7].

3.2. Distribution of total strain and translational displacement

The maximum deformation occurs on the tube wall opposite the clamping region, due to a springback effect when the material is subjected to eccentric loading. The peak displacement is recorded at approximately [value].

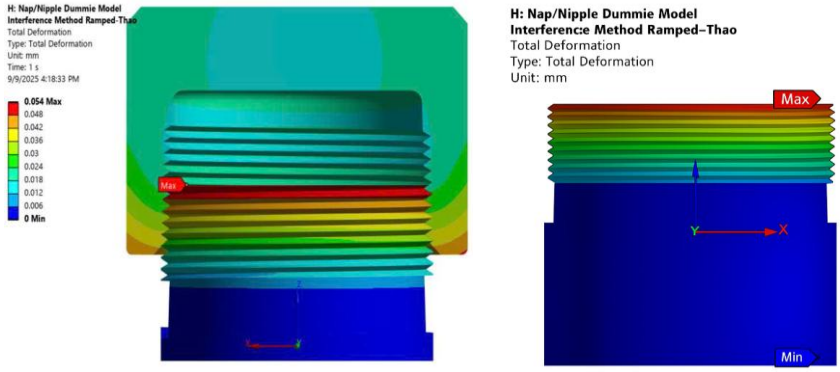

(a) *(b)*

Figure 4. *Effect of clamping force on the stress state of the threaded joint. (a) Clamping force 2 kN; (b) Clamping force 3 kN.*

The asymmetric displacement distribution around the tube circumference leads to loss of circularity, thereby reducing the sealing capability of the threaded joint, particularly under liquid or gas pressure.

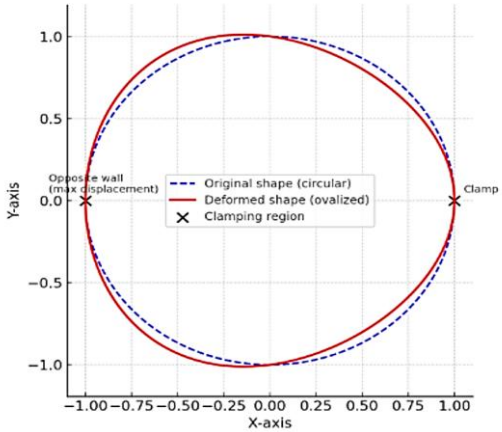

Figure 5. *Ovalization of the tube cross-section under clamping force.*

3.3. Analysis of the Influence of Clamping Force and Torque

The clamping force F has a dominant effect on the overall stress level and deformation of the thin-walled tube. As F increases from 1.5 to 3.0 kN, the maximum Von Mises stress rises almost linearly up to 2.0 kN, followed by a nonlinear increase beyond this threshold due to local yielding at the thread roots and clamp–tube contact zone. When F > 2.0 kN, the plastic strain becomes

noticeable, and the tube shows partial ovalization near the clamping area. Quantitatively, the stress increases from 235 MPa at 1.5 kN to 390 MPa at 3.0 kN, corresponding to an approximate 66% growth, confirming that excessive clamping may induce permanent deformation. Therefore, the safe clamping limit is recommended at F ≤ 2.0 kN.

The applied torque M primarily influences the shear stress distribution and local stress concentration at the thread flanks. When M increases from 10 N·m to 25 N·m under a fixed clamping force of 2 kN, the maximum Von Mises stress rises moderately from 285 MPa to 340 MPa (≈ 19% increase). However, the stress pattern shifts circumferentially, indicating stronger tangential loading at the upper thread region. The torque also contributes to micro-sliding at the contact interface, intensifying frictional heating and local strain, but its overall effect remains secondary compared with the clamping force. This confirms that F governs axial compression and deformation, while M mainly alters local shear response.

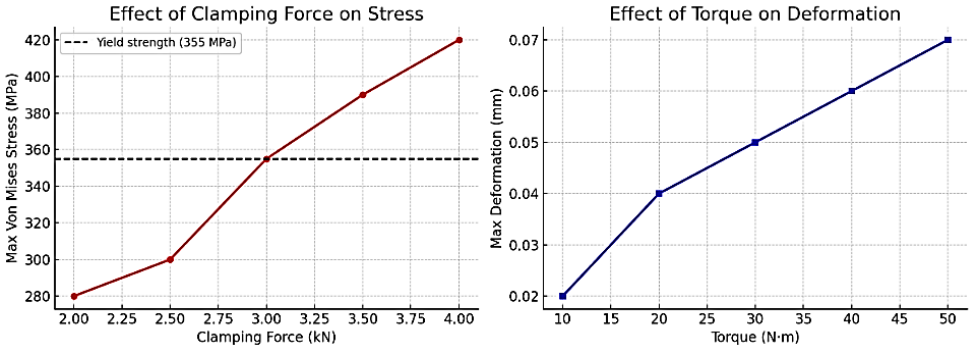

Figure 6. *Factor of safety (FOS) distribution in the threaded joint.*

3.4. Analysis of the factor of safety

To assess the safety level of the threaded joint under standard working conditions, the factor of safety is calculated as follows: $F_{OS} = \frac{\sigma_y}{\sigma_{\max}} = \frac{355MPa}{310MPa} \approx 1.15$. The obtained FOS value is relatively low and does not meet the conventional design requirement in mechanical engineering, which typically demands $F_{OS} \geq 1.5$.

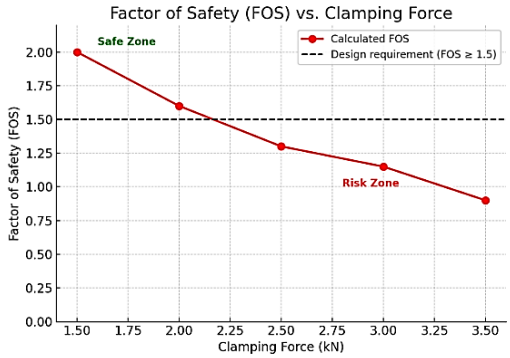

Figure 7. *Factor of safety (FOS) distribution in the threaded joint.*

Implication: With F_{OS} < 1.5, the structure is highly susceptible to damage under load fluctuations or assembly errors. Therefore, several engineering solutions should be applied: Increase the wall thickness in the threaded region; Use tubes made of higher-strength materials; Optimize the geometry of the thread–clamp contact zone; Limit clamping force within the safe range (< 2.5 kN).

3.5. Proposed solutions and practical applications

The simulation and analysis results show that, to ensure that the Von Mises stress in the C45 steel tube does not exceed the yield strength (σy = 355 MPa), the maximum allowable clamping force must not exceed 2.0 kN. If the clamping force is greater than 2.5 kN, irreversible plastic deformation occurs at the thread roots and the clamp–tube contact region, reducing the tightness and service life of the joint.

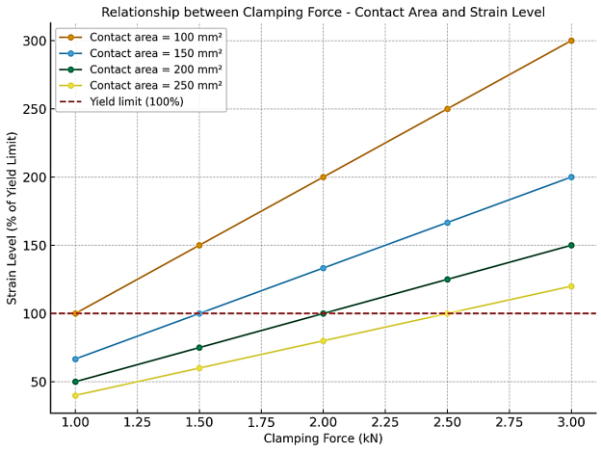

Figure 8. *Proposed design improvements for enhancing the strength of threaded joints.*

In addition, the contact area between the clamp jaws and the tube wall should be at least 150–200 mm² to distribute the load evenly and reduce stress concentration at the clamping zone. When the contact area is smaller than this threshold, the surface pressure exceeds 12 - 15 MPa, which can easily cause local deformation and ovalization of the tube during assembly/disassembly.

The simulation results can be effectively applied in the design and maintenance of piping systems, where they provide a scientific basis for inspection and routine servicing. Specifically, the defined clamping force limit and required contact area serve as crucial parameters for establishing safe tightening standards. These standards can be applied to both automatic and manual assembly/disassembly tools, thereby preventing structural damage during operation and ensuring the long-term reliability of threaded joints.

3.6. Verification & validation

3.6.1. Verification – numerical solution verification

Objective: To evaluate discretization error and assess the reliability of FEM results in critical regions (thread roots and clamp–tube contact zones).

Setup: All modeling conditions remain identical to the original simulation (material σ_y ≈ 355 MPa, nonlinear frictional contact μ ≈ 0.15, Augmented Lagrange formulation, fixed–free boundary, applied F and M). A controlled mesh refinement was performed with second-order SOLID187 elements at the thread root and clamp–contact zones: Coarse mesh: local element size $h_1 \approx 0.35$ mm; Medium mesh: $h_2 \approx 0.25$ mm; Fine (reference) mesh: $h_3 \approx 0.20$ mm (used in the paper). Maximum von Mises stress $\sigma_{v,\max}$ max at the thread root, and the maximum equivalent strain $\varepsilon_{eq,\max}$ on the opposite tube wall.

GCI procedure (ASME V&V 20, Richardson extrapolation):

- Compute refinement ratios $r = h_2/h_1$ and h_3/h_2 (≈ 0.71 and 0.80).

- From three mesh solutions ϕ_1, ϕ_2, ϕ_3 determine the observed order of convergence p and the Richardson-extrapolated value ϕ_{ext}.

- Compute fine-grid uncertainty.

$$\mathrm{GCI}_{\mathrm{fine}} = \frac{F_s \mid \phi_3 - \phi_2 \mid}{\phi_3(r^p - 1)} \times 100\%,\ F_s = 1.25$$

- Report $\phi_3 \pm \mathrm{GCI}_{\mathrm{fine}}$ as the numerical confidence interval.

Recommended: Include a table (mesh size h, number of elements, $\sigma_{v,\max}$, $\varepsilon_{eq,\max}$ p, GCI). For SOLID187 (quadratic), p ≈ 2.0 and GCI < 5% indicate reliable convergence.

Contact algorithm sensitivity: Repeat the fine mesh with ± 20 % variation in normal stiffness and penalty factor (Augmented Lagrange). If the resulting $\sigma_{v,\max}$ changes < 3 - 5%, the contact algorithm is numerically stable. Friction sensitivity: Vary μ = 0.10–0.20 (step 0.025) and compute $\partial\sigma_{v,\max}/\partial\mu$. If sensitivity is low (≤ 5%) at F = 2 kN, μ = 0.15 is acceptable for dry contact conditions [8].

3.6.2. Validation – comparison with analytical model

The thin-walled tube (D = 114 mm → r = 57 mm, t = 2 mm) is subjected to (i) localized clamping pressure $p = F/A$ on an effective contact area A, and (ii) torsional moment M uniformly distributed along the circumference.

- Hoop and axial stresses:

$$\sigma_\theta \approx -\frac{pr}{t}, \sigma_z \approx -\frac{pr}{2t}$$

Negative sign denotes compression.

- Shear stress due to torque (Bredt–Batho thin-tube formula):

$$\tau \approx \frac{M}{2\pi r^2 t}$$

- Combined von Mises stress:

$$\sigma_v = \sqrt{\frac{(\sigma_\theta - \sigma_z)^2 + (\sigma_z - 0)^2 + (0 - \sigma_\theta)^2}{2} + 3\tau^2}$$

Given F = 2.0 kN, M = 20 N·m, and effective contact area A = 150 - 200 mm^2:

A (mm²)	p (MPa)	σ_θ (MPa)	σ_z (MPa)	τ (MPa)	σ_v^(th) (MPa)
200	10.0	−285	−142.5	0.49	247
150	13.3	−380	−190	0.49	329

FEM comparison: At the same load (F = 2 kN, M = 20 N·m), simulation gives $\sigma_{v,\max} \approx 310$ MPa at the thread root/contact region. The analytical range (247–329 MPa) encloses this value, closely matching A ≈ 150 mm^2 (≈ 6% deviation). Thus, FEM and analytical predictions are quantitatively consistent, the FEM captures local peaks higher than shell-averaged analytical stresses. Validation result: Agreement within 6 - 25% depending on A; minimum deviation occurs at A ≈ 150 mm². This confirms both the location and magnitude of stress concentration and validates the proposed safe clamping range. Solving $\sigma_v^{(th)}(F,A,M=20) = \sigma_y$ (≈ 355 MPa):

Compared with FEM (onset of yielding at ≈ 2.0–2.5 kN), the analytical prediction is very close (difference ≈ 7 - 15%). Hence, the operational recommendation F ≤ 2.0 kN - particularly for A < 200 mm² due to wear or misalignment, is conservative and valid. Maintaining A ≥ 150 - 200 mm² increases the safety margin.

3.6.3. Summary of V&V and uncertainty

Verification: Mesh refinement with SOLID187 provides GCI < 5% for $\sigma_{v,\max}$; contact and friction sensitivities are minor (< 5%). → Numerically stable solution. Validation: Analytical thin-shell + Bredt model agrees quantitatively with FEM; the theoretical yield clamping limit matches

FEM trend. Main uncertainty sources: (i) Approximating localized clamp load as uniform pressure; (ii) geometric tolerances and surface roughness at threads; (iii) friction variation with lubrication/environment; (iv) actual stiffness of clamp assembly.

Recommended presentation: Include (1) mesh-convergence + GCI table, (2) comparison table FEM vs analytical at F = 2 kN (M = 20 N·m, A = 150/200 mm²), (3) stress–force plots, and (4) emphasize safe operation range F ≤ 2 kN, A ≥ 150 - 200 mm².

4. CONCLUSIONS

Finite element simulations have shown that stress concentration mainly occurs at the thread root and the clamp–pipe contact region. When the clamping force exceeds 2.5 kN or the contact area is too small (<150 mm²), the stress surpasses the yield limit, leading to plastic deformation and a reduction of the factor of safety (FOS ≈ 1.15).

Therefore, to ensure safety and extend the service life of threaded joints in thin-walled steel tubes, it is necessary to: Keep the clamping force ≤ 2.0 kN; Ensure the clamp contact area is ≥ 150–200 mm²; Apply optimized design measures such as increasing tube wall thickness, selecting higher-strength materials, and improving thread geometry.

REFERENCES

[1]. Shigley, J. E. and C. R. Mischke, *"Mechanical Engineering Design"*, McGraw-Hill, (2002).
[2]. ANSYS Inc., *"ANSYS Mechanical User's Guide"*, ANSYS Inc., (2021).
[3]. ISO, *ISO 965-1:1998 — "ISO Metric Screw Threads – General Plan"*, International Organization for Standardization, (1998).
[4]. Boresi, A. P. and R. J. Schmidt, *"Advanced Mechanics of Materials"*, Wiley, (2003).
[5]. Zhang, J.-Y., W.-G. Zhang, and Y.-F. Zhou, *"Analysis of mechanical strengths of extreme line casing joint considering geometric, material, and contact nonlinearities"*, Petroleum Science and Engineering Journal, (2024).
[6]. Liu, C., T. Zhang, and S. Zhang, *"A new threaded insert reinforced joint to achieve ultra-high performance in CFRP bolted connections"*, Composites Part B: Engineering, 295, (2025).
[7]. Abdullah, N. A., J. S. Han, and M. A. Ismail, *"Finite element modelling approaches for sheet metal joining"*, Proceedings of the IMechE, Part C: Journal of Mechanical Engineering Science, (2024).
[8]. Zhu, Y. et al., *"Experiment and finite element research on mechanical performance of thin-walled steel–wood composite columns under eccentric compression"*, Buildings, 15, 12, 2114, (2025).

TÓM TẮT

Phân tích biến dạng của ống thép mỏng dưới lực kẹp khi tháo lắp mối ghép ren bằng phương pháp phần tử hữu hạn

Các mối ghép ren trên ống thép thành mỏng được sử dụng rộng rãi trong các ứng dụng công nghiệp, nơi việc tháo lắp nhiều lần có thể dẫn đến biến dạng cục bộ và suy giảm độ bền của chi tiết. Nghiên cứu này sử dụng phương pháp phần tử hữu hạn (FEM) để phân tích ứng xử ứng suất – biến dạng của ống thép thành mỏng dưới tác dụng đồng thời của lực kẹp và mô men xoắn. Trong mô hình mô phỏng, tiếp xúc phi tuyến có ma sát và tính dẻo của vật liệu được xem xét nhằm mô phỏng điều kiện biên thực tế. Kết quả cho thấy ứng suất tập trung chủ yếu tại chân ren và vùng tiếp xúc giữa ngàm kẹp và ống. Biến dạng dẻo bắt đầu xuất hiện khi lực kẹp vượt quá 2 kN. Dựa trên kết quả mô phỏng số, nghiên cứu đề xuất giới hạn lực kẹp an toàn và khuyến nghị thiết kế nhằm ngăn ngừa chảy dẻo và đảm bảo độ tin cậy kết cấu của mối ghép ren.

Từ khóa: Ống thép mỏng; Mối ghép ren; Lực kẹp; Phương pháp phần tử hữu hạn; Biến dạng cục bộ; ANSYS.